Available online at http://www.ijprt.org.tw/

Chinese Society of Pavement Engineering

International Journal of Pavement Research and Technology 11 (2018) 846-860

http://www.ijprt.org.tw/

Horizontal deformation resistance of paving block superstructures – Influence of paving block type, laying pattern, and joint behaviour

H.L. Hengl [a], W. Kluger-Eigl [b], M. Lukacevic [a], R. Blab [b], J. Füssl [a,*]

[a] Institute for Mechanics of Materials and Structures, TU Wien, Austria
[b] Institute of Transportation, TU Wien, Austria

Received 30 November 2016; received in revised form 21 June 2018; accepted 9 August 2018

Abstract

Paving block structures are experiencing an upswing in urban areas, mainly due to their ecological, economical and space forming qualities. Unfortunately, this trend is being weakened by damages which occur even if all design standard were met. Very often unsightly horizontal relative deformations between paving blocks are observed, a failure mechanism which is not taken into account in standards sufficiently.

The identification and assessment of such horizontal deformation mechanisms of paving block superstructures represents the main objective of the present work. This is realized by means of complex 3D finite element simulations, investigating six different laying patterns with five different types of paving blocks, resulting in a strongly different joint behaviour of each configuration. The non-linear interaction behaviour between paving blocks was identified experimentally, implemented into the numerical simulation tool, and subsequently allowed for the reproduction of very realistic horizontal deformation mechanisms.

Finally, the performance of several laying pattern and paving block type configurations were compared to each other, pointing out the strength and weaknesses of each superstructure and revealing which combinations are performing best.
© 2018 Chinese Society of Pavement Engineering. This is an open access article under the CC BY-NC-ND license (http://creativecommons.org/licenses/by-nc-nd/4.0/).

Keywords: Horizontal loading; Block pavements; Finite elements analysis; Numerical simulation

1. Introduction and motivation

Paving block structures are experiencing an upswing in urban areas due to their ecological, economical and space forming qualities compared to common asphalt pavements. Even in areas with high traffic volumes paving block structures are expected to represent a suitable alternative to common pavement building systems in future. This trend is, however, continuously weakened by unexpected damage of newly built paving block pavements. The reason for this are immature design concepts and standards, which are heavily based on the concepts for asphalt pavements and do not take the special characteristics of this block-like structures sufficiently into account. The success of a project is therefore strongly dependent on the quality of planning and construction provided by experienced engineers and executing companies, rather than on reliable scientific knowledge implemented into design concepts and standards.

A brief overview of the rather modest research activities concerning paving block structures is given in the following. One of the first investigations on paving block structures with finite element simulations were done by Nishizawa et al. [1] in 1984. He developed a numerical model with the joints modelled through a set of springs and 2D rectangular plate elements. In 1988 Jacobs and Houben [2] undertook further investigations using 2D rigid

* Corresponding author.
E-mail address: Josef.Fuessl@tuwien.ac.at (J. Füssl).

https://doi.org/10.1016/j.ijprt.2018.08.001
1996-6814/© 2018 Chinese Society of Pavement Engineering.
This is an open access article under the CC BY-NC-ND license (http://creativecommons.org/licenses/by-nc-nd/4.0/).

block elements connected with linear springs. The first 3D finite element approach can be found in Huurman [3], where the numerical model contains paving blocks interconnected by four sets of three springs for each joint. The paving block superstructure is placed on four layers of bedding and subject to vertical loading. Displacement, stress, and strain information for the paving blocks, as well as for the baselayers and subgrade could be obtained. Higher bending stresses were determined in case of higher joint stiffness. Hassani [4] used shell elements to model paving blocks and the joints between them. Lerch [5] and Ascher et al. [6] implemented a non-linear interaction between paving blocks, represented by zero-thickness elements in their simulations, where elastic as well as shear moduli were adjusted iteratively during the analysis. Later, this interactions were substituted by non-linear contact laws, allowing for elastic–plastic interactions between paving blocks. Also Nejad and Shadravan [7] modelled interactions with contact elements and found out that jointing width, shape, size, and thickness of the paving blocks have a major impact on the vertical structural deformations. Mampearachchi and Gunarathna [8] performed a parametric study under usage of a 3D finite element model to determine necessary improvements for weaker support conditions of paving block structures. In the work of Oeser and Chandra [9] a 3D Cosserat theory is applied to a sophisticated computational model using elastic as well as plastic interaction properties. A 3D numerical simulation tool for concrete paving slabs is presented in Füssl et al. [10–12], where non-linear and plastic behaviour between paving slabs and between slabs and sandbed is taken into account. In Hengl and Füssl [13] various parameter studies were carried out on comprehensive numerical models to define an optimal region of superelevation-to-road-width ratios for superelevated profiles of paving block structures, and in Hengl et al. [14] the temperature loading on paving block superstructures is investigated numerically.

The main focus of all these research lied on the vertical structural response of paving block structures and the critical stresses and strains in the underlying baselayers. In addition to the vertical resistance, however, the structural resistance to horizontal loads is assumed to represent an equally important performance characteristic, especially for paving block structures. According to experienced engineers, it is often observed in practice that due to braking and steering manoeuvre of heavily loaded trucks or buses damage is introduced into paving block structures. Such loadings are normally not part of design approaches and also hardly treated in scientific literature. An interesting experimental work is presented in Rachmat et al. [15], investigating the horizontal performance of paving block pavement on sloped road sections. Neglecting these horizontal loadings can cause damage in form of permanent shiftings in the superstructure and chipped edges of paving blocks, as can be seen in Fig. 1.

For example, the Austrian regulation for paving block pavements RVS 03.08.63 defines the admissible paving block structure as well as the thickness of the base courses only based on the expected traffic volume. However, it is obvious that the paving block surfaces, the shape, as well as the laying pattern must have a significant impact on the horizontal shifting resistance (responsible for frequently observed shortcomings) of the superstructure. This represents the main motivation for this work, which aims at a numerical simulation tool able to capture the effect of different laying patterns as well as different types of

Fig. 1. Damage in a paving block structure because of too little horizontal loading resistance.

paving blocks on the horizontal shifting resistance of the related paving block superstructure. Based on this motivation, the following main objectives had been defined:

- The definition of sufficiently large and suitable submodels of paving block superstructures allowing for the determination of the horizontal shifting resistance of these structures without significant influence of the boundary conditions. Furthermore, an automated generation of the whole superstructures' geometry, to allow for an efficient investigation of several paving block geometries as well as laying patterns.
- An appropriate description of the non-linear interaction behaviour, in tangential as well as normal direction of the vertical joints, between paving blocks. Shear failure in the joints and the opening of joints should be reproduced realistically.
- Finally, the finite-element-based determination of the horizontal shifting resistance as well as the corresponding deformation (failure) mechanisms of different paving block superstructures.

The 5 types of paving blocks and the 6 different laying patterns investigated in this work are shown in Fig. 2. To get realistic interaction properties, describing the contact behaviour between paving blocks, two types of experiments on paving blocks were carried out. The experimental setup as well as the results are given in Section 2. In Section 3, the developed simulation tool is described in and the corresponding numerical results are presented in Section 4. Thereby, each paving block was examined in every type of laying pattern. Finally, concluding remarks are given in Section 5.

2. Identification experiments for the vertical joint behaviour

The transmission of forces between paving blocks through the vertical joints of the paving block structure strongly affect, not to say define, the overall structural behaviour in horizontal direction. For this reason, special focus was laid on the identification of these properties. Two different kinds of experiments were carried out at the TVFA Vienna to obtain shear and normal properties for all of the 6 paving block types aforementioned. The experiments and the results are presented in the following two subsections. Additional information about such experiments can be found in Füssl et al. [16], where similar tests were performed by the authors.

2.1. Normal joint behaviour experiment

The experimental setup for the identification of the joint behaviour in normal direction is illustrated in Fig. 3. Thereby, two paving blocks are placed on a wooden multilayer board and the 5 mm thick joint between them is filled with sand (0/2) and manually compacted. One paving block is completely clamped while to the other one a horizontal force H is applied and the relative normal displacement u_n between these two blocks is measured with an LVDT. The obtained relationships between the normal

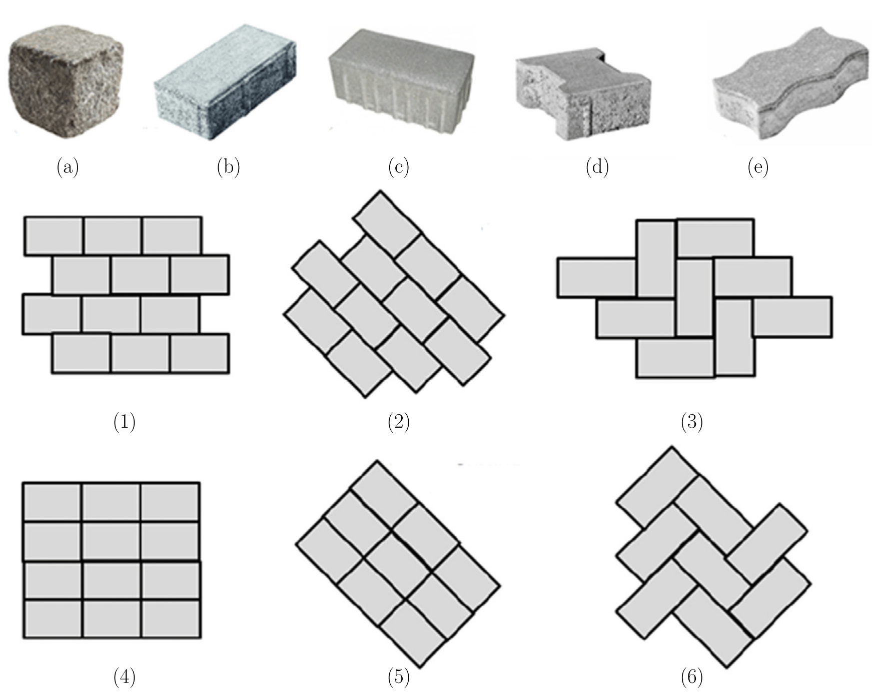

Fig. 2. Paving block types and laying patterns investigated in this work: (a) Granite Cube, (b) Concrete Block, (c) Concrete Interlocking Block (CIB), (d) Double-T Block, (e) Wave Block, and (1) Stretcher Bond, (2) Stretcher Bond 45°, (3) Herringbone, (4) Stacked Bond, (5) Stacked Bond 45°, (6) Herringbone 45°.

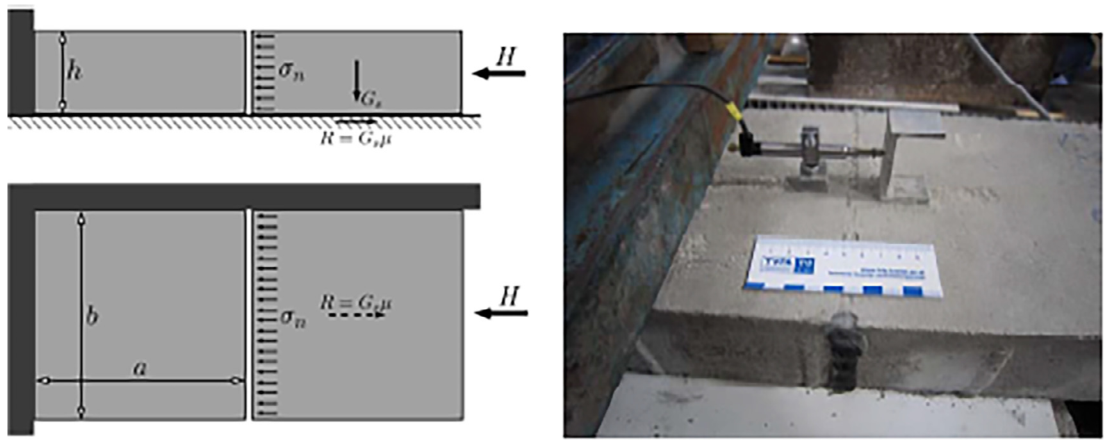

Fig. 3. Experimental setup for the identification of the joint behaviour in normal direction.

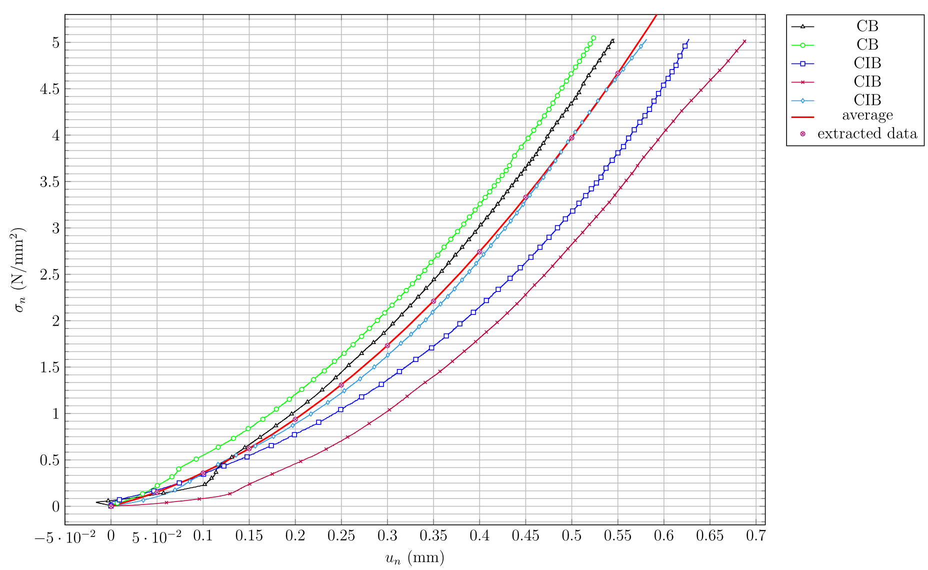

Fig. 4. Relationships between the normal stress σ_n in the vertical joints and the relative displacement u_n between paving blocks (Concrete Blocks and Concrete Interlocking Blocks) obtained from experiments.

stress σ_n and the displacement u_n for 5 performed tests are plotted in Fig. 4. Since this information was assumed not to be as decisive as the shear behaviour and less dependent on the type of paving block, this experiment was only conducted with Concrete Blocks and Concrete Interlocking Blocks. Finally, an average response was evaluated (red graph in Fig. 4), from which the input data for the numerical simulation tool were extracted (given in Table 1).

2.2. Tangential joint behaviour

The experimental setup to identify the tangential joint behaviour is illustrated in Fig. 5. Thereby, three paving blocks are arranged in a row on a wooden multilayer board and the 5 mm thick joints in-between are filled with sand (0/2), which is mechanically compacted under dry conditions. Then, in a first step, a constant load H is applied

Table 1
Average normal joint behaviour extracted from the experimental results shown in Fig. 4, used as input to the numerical simulation tool.

Deformation u_n [mm]	Pressure σ_n [MPa]
−0.5	0
0	0.0001
0.05	0.15143
0.1	0.35921
0.15	0.62114
0.2	0.93722
0.25	1.30745
0.3	1.73183
0.35	2.21036
0.4	2.74304
0.45	3.32987
0.5	3.97085
0.55	4.66598

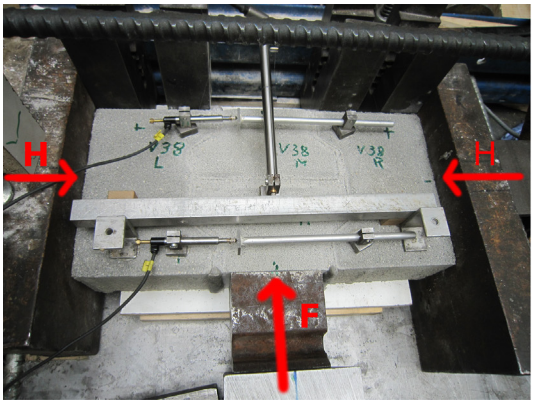

(a) Double-T Block, Initial (undeformed) configuration.

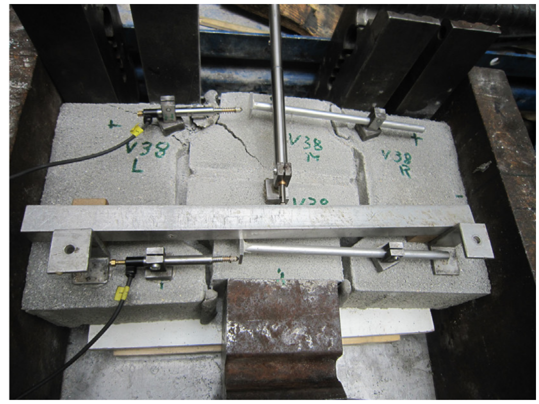

(b) Double-T Block, Exemplarily state after failure.

(c) Concrete Block, Initial (undeformed) configuration.

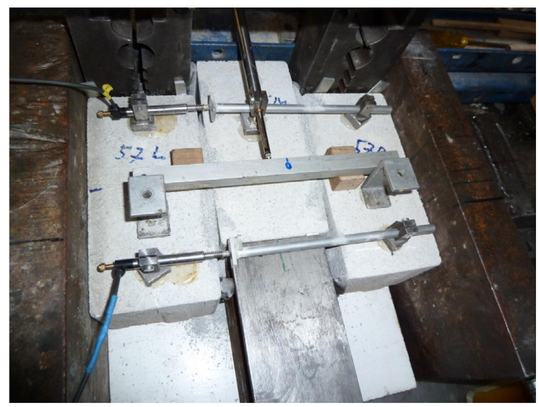

(d) Concrete Block, Exemplarily state after failure.

(e) Wave Block, Initial (undeformed) configuration.

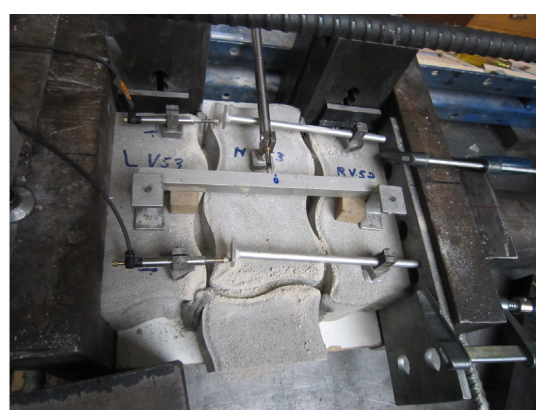

(f) Wave Block, Exemplarily state after failure.

Fig. 5. Experimental setup to identify the tangential joint behaviour for (a,b) the Double-T Block, (c,d) the Concrete Block, and (c,f) the Wave Block.

in "row"-direction (horizontal direction in Fig. 5), allowing frictional forces to be activated in the joints. In a second step, an increasing load F is applied to the middle paving block transversely to the "row"-direction up to the point of shear failure (see, e.g., Fig. 5(b, d, f)). The relative displacements in "row"-direction as well as the force F were measured continuously. This experiment was carried out for all 5 types of paving blocks, at each for up to 5 different constant loads H and with at least two tests per configuration to ensure repeatability. For all these tests the

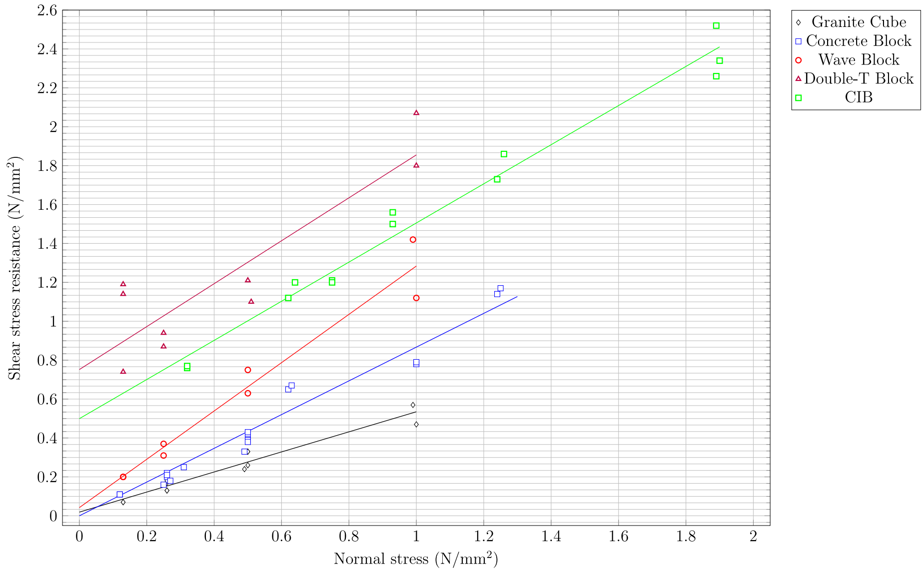

Fig. 6. Shear stress resistance – Results of horizontal displacement experiments.

Table 2
Mohr–Coulomb friction parameters for all 5 paving block types obtained from identification experiments.

Specimens	Dimension [cm]	Cohesion c [MPa]	Friction angle [°]
Concrete Block	20/10/8	0	49.69
Granite Cube	18/18/18	0.0189	29.56
Wave Block	21.5/10.5/8	0.0422	71.15
CIB	20/10/8	0.4994	57.64
Double-T Block	19.5/16/7.6	0.7519	63.23

maximum (average) shear stress in the joint as a function of the average normal stress in the joint, defined through the load H, is plotted in Fig. 6.

The data of each paving block type can be connected through a Mohr–Coulomb friction law quite well (linear graphs in Fig. 6). The resulting Mohr–Coulomb friction parameters (cohesion and friction angle) for each paving block type are given in Table 2, and were subsequently used as input to the numerical simulation tool.

3. Numerical simulation tool

Exemplarily for all models of different laying patterns, the model for a stretcher bond 45° is displayed in Fig. 7. It only consists of the paving blocks and the underlying sandbed. The other base layers were not modelled explicitly, since it can be assumed that they contribute only little to the horizontal shifting resistance of the whole paving block structure. At least they would not influence the performance comparison between different paving blocks and laying patterns, which is the main focus of this work. For all models the chosen modelling area is rectangular with an approximate dimension of 5.8 m to 2.6 m. Small deviations to this dimensions result from the different laying patterns. The dimensions of the paving blocks are set, according to an industry standard, to 200/100/100 mm. Paving blocks with different geometry and dimensions are used as border stones to provide a straight boundary. Linear elastic material behaviour is assigned to the paving blocks, with an elastic modulus of 45 000 MPa, which was obtained by ultrasonic experiments on similar paving blocks in Füssl et al. [11], and a poisson's ratio of 0.15. Furthermore, a specific weight of 24 kN/m^3 was assumed for the paving blocks, allowing to take their dead load within the simulations into account.

The interaction between paving blocks in normal direction is defined as a tabular pressure–overclosure relationship according to the normal joint behaviour experiments described in Section 2, whereas the exact values used can be found in Table 1. The interaction behaviour in tangential direction between paving blocks is described by a Mohr–Coulomb friction law, with the cohesions and friction angles obtained from the tangential joint behaviour experiments described in Section 2. For all investigated paving blocks these strength values can be found in Table 2. The default Mohr–Coulomb friction criterion in Abaqus is not able to take a cohesion not equal to zero into account. For this reason, this criterion has been adapted and implemented as a user subroutine written in Fortran. More details of the implementation of this tangential behaviour

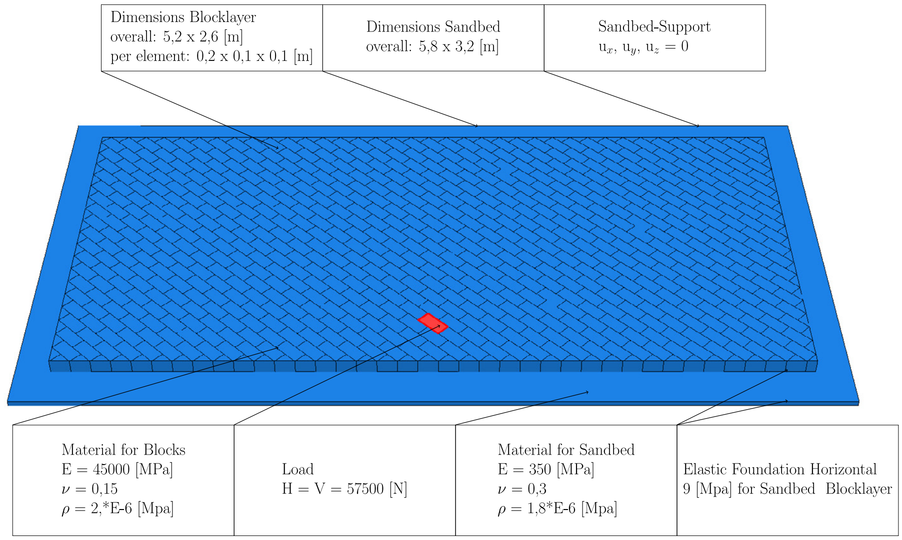

Fig. 7. Geometry and boundary conditions of the numerical model illustrated by means of a stretcher bond 45° model.

will be given in a following subsection. At the lateral boundary all paving blocks are supported by an elastic foundation with a bedding modulus of 9 MPa/mm, which is an extrapolated value obtained from the normal pressure–displacement relationship in Fig. 4. This bedding modulus approximately represents the stiffness of a vertical sand joint adjacent to a rigid border block.

To the underlying sandbed also a linear elastic material behaviour has been assigned, with an elastic modulus of 350 MPa, a Poisson's ration of 0.3 and a specific weight of 18 kN/m^3. Since the vertical structural response of the paving block structure was not investigated in this work it seemed not to be necessary to model a more complex behaviour. For this reason, also the displacements of the lower surface of the sandbed were simply prevented in all spacial directions. Between the sandbed and the paving blocks a "hard" contact was assumed in normal direction, allowing the paving blocks to lift off unstressed while stresses are transmitted fully under pressure. In tangential direction classical Mohr–Coulomb friction is modelled with a frictional coefficient of 0.6 and no cohesion.

The whole model is discretised with 8-node hexahedron elements, except some of the border blocks with non-rectangular geometry where wedge elements are used. Exemplarily, the discretised version of the stretcher bond 45° model is shown in Fig. 8. A characteristic mesh size of 25 mm is used for the paving blocks, whereas the mesh is refined (12.5 mm characteristic mesh length) in the area where the wheel-load is applied. The horizontal element lengths of the mesh of the sandbed is 50 mm, finally resulting in a total number of elements for each model of around 100 000.

The simulations were carried out as follows: In a first analysis step the dead load and in a second analysis step a fictitious braking performance of a single tire was applied to a single paving block. This fictitious loading consists of a standard vertical tire load of 57.5 kN and of a horizontal loading of equal size, representing an absolute upper limit of possible braking forces. The finite element analysis was carried out with the Abaqus/Standard solver on a HPC computing cluster at TU Wien, using unsymmetrical matrix storage and including non-linear effects of large displacements.

To improve the stability of the numerical simulations an elastic slip at all tangential contact interactions was allowed. However, this elastic slip was restricted to 0.0005 times the adjacent characteristic element size l_{el} and therefore has no significant influence on the numerical

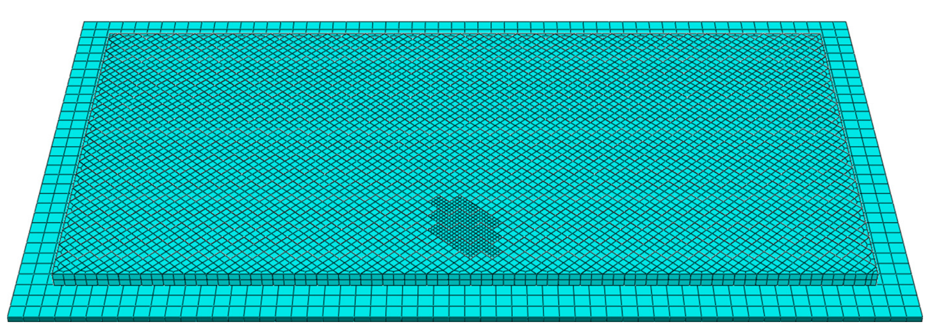

Fig. 8. Discretisation of the stretcher bond 45° model with 8-node hexahedron elements.

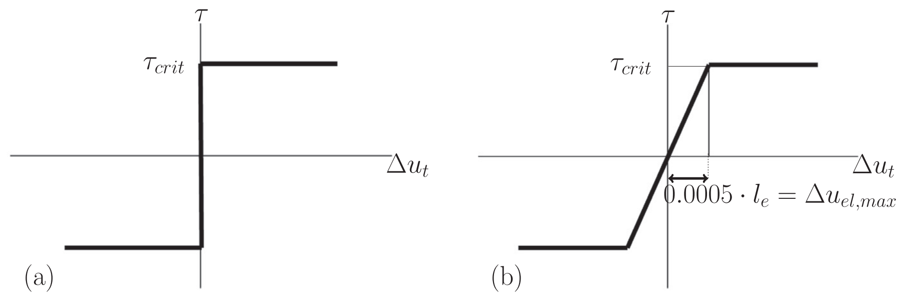

Fig. 9. (a) Ideal frictional behaviour and (b) the approximation allowing a small amount of elastic slip used in this work.

result. The ideal frictional behaviour, where no relative motion Δu_t is allowed for $|\tau| < \tau_{crit}$, as displayed in Fig. 9 (a) is thus approximated with the relationship shown in Fig. 9(b). So, a small amount of elastic motion, related to the frictional shear stress through:

$$\Delta u_{el} = \frac{\tau_{crit}}{\Delta u_{el,max}} \cdot \Delta u_t = \frac{0.6 \cdot \sigma_n}{0.0005 \cdot l_e} \cdot \Delta u_t : \{\Delta u_t \in \mathbb{R} \mid |\Delta u_t| \leqslant \Delta u_{el,max}\},$$

where σ_n represents the pressure between paving block and sandbed, is allowed. For more detailed information about the numerical implementation of Mohr–Coulomb friction using the penalty method, which was used in this work, the reader is referred to Corp. [17].

3.1. Creation of different model geometries

Due to the large number of paving blocks modelled for each laying pattern (as can be seen in Fig. 7) and to be able to flexibly adjust geometric parameters the models were generated by an extensive python script consisting of more than 1000 lines of code. The script offers a GUI through which future users can define a variety of parameters, such as the dimensions of the paving block, the size of the model region, the material and contact properties, as well as the type of laying pattern. Subsequently, the whole model is generated automatically, including the geometry of the border stones and all the contact interactions between the paving blocks and the paving blocks and the sandbed. Furthermore, in combination with a bash script this automated model generation provides a powerful tool for conducting parameter studies.

4. Numerical simulation results

As already mentioned within the introduction, numerical simulations have been performed for each configuration of the 5 different paving blocks and the 6 different laying patterns proposed, with the intention to determine the effect of those on the horizontal shifting resistance of the corresponding paving block superstructure. Trying to present the results in a structured way, in the first subsection the performance of all 5 paving blocks is compared by means of two laying patterns, while the performance of the 6 different laying patterns is compared in the second subsection by means of only the Concrete Block and the Concrete Interlocking Block. Finally, a result overview of all simulations conducted is given in the third subsection.

4.1. Performance of different paving blocks arranged in the same laying pattern

Fig. 10 shows the horizontal deformation fields for all 5 different paving blocks laid in a stacked bond. For comparison reasons all paving blocks were modelled with the same dimensions. In addition, it should be noted here that since the non-planar side surfaces of the Double-T Block as well as the Wave Block are already considered within the identified strength parameters obtained from experiments, the real geometry of these paving blocks doesn't need to, or even must not, be modelled at this structural scale.

For the visualisations in Fig. 10 the sandbed was excluded and the deformations were scaled by a factor of 100. All deformation fields are related to the same fictitious loading state as described before and, thus, show an impressive performance difference between these five different paving blocks. For the Concrete Block, exhibiting zero cohesion between paving blocks, about six times the deformation was obtained compared with the best-performing Double-T Block. Since there are no compressive stresses in transverse direction, the Concrete Block is not able to transfer shear stresses to adjacent rows and, thus, only the loaded row is shifted in load direction. The maximum displacement could be obtained by simply summing up the overlaps of the paving blocks in this row, which can be interpreted as the compression of the sand joints plus the displacement of the border block of the structure, which is kept quite small by a relatively stiff elastic foundation on the boundary. It can be assumed that the maximum displacement would be even larger if more paving blocks were modelled in load direction. A similar picture is drawn by the Granite Cube, also exhibiting only a very small cohesion of 0.019 MPa. For this reason, as expected, paving blocks with no interlocking effect (cohesion) are not suitable for this laying pattern. A completely different system response was obtained for the three paving blocks having significant interlocking capabilities, the Wave Block,

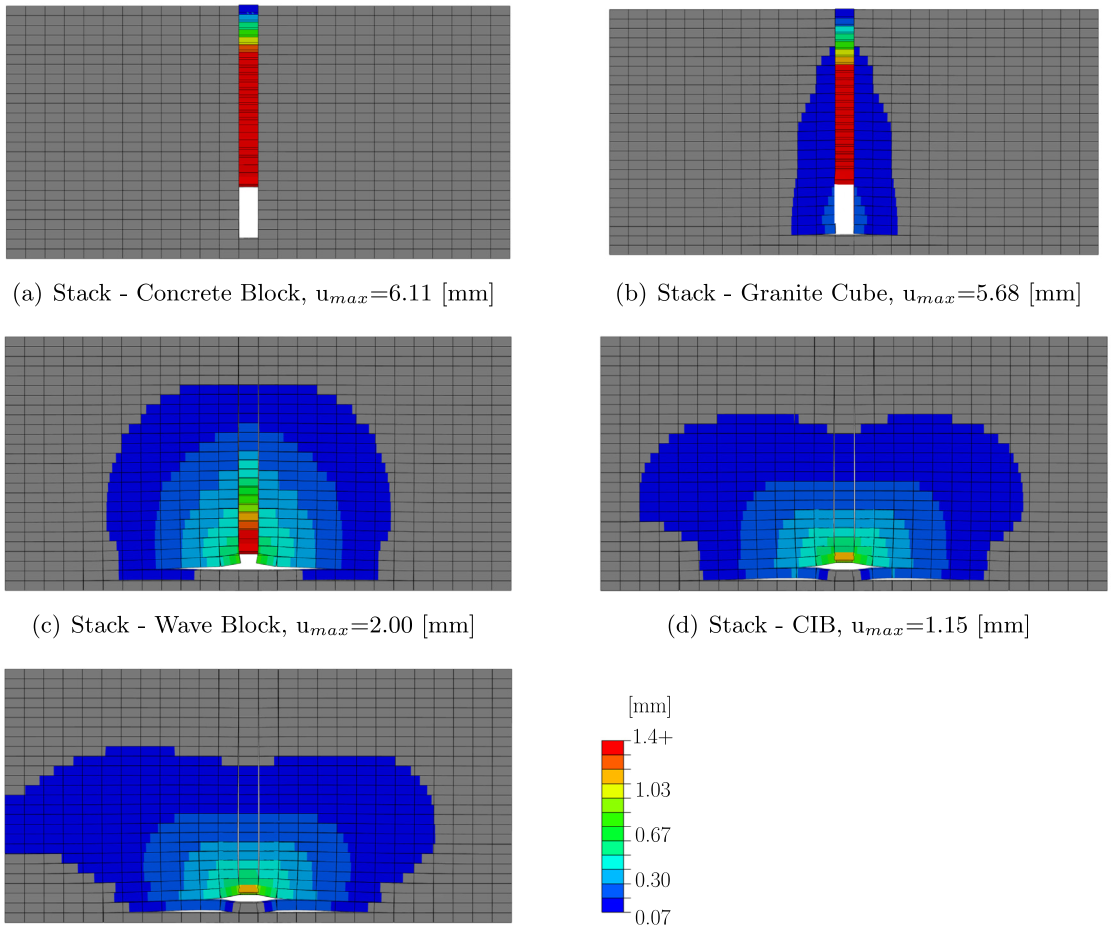

(a) Stack - Concrete Block, u_{max}=6.11 [mm]

(b) Stack - Granite Cube, u_{max}=5.68 [mm]

(c) Stack - Wave Block, u_{max}=2.00 [mm]

(d) Stack - CIB, u_{max}=1.15 [mm]

(e) Stack - Double-T Block, u_{max}=1.08 [mm]

Fig. 10. Horizontal deformation fields of the 5 investigated paving blocks arranged in a stacked bond. A vertical and horizontal load of 57.5 kN each is introduced on one paving block. Scaling of deformations: 100.

the Concrete Interlocking Block, and the Double-T Block. For all three, the obtained displacement field was proven to be independent on the boundary conditions, and without any compressive force in transverse direction they are able to activate a large amount of paving blocks counteracting the very concentrated introduced load.

This can also be seen very clearly in Fig. 11, in which the normal and shear contact forces between paving blocks are vividly illustrated, for the Concrete Blocks and the Concrete Interlocking Blocks.

The great decrease in contact forces in the surrounding of the load introduction comes from the great shear forces which can be transferred to the sandbed by the paving blocks which experience a substantial vertical loading. At a certain distance from the load introduction a constant decrease in contact forces can be observed, reflecting the shear transfer capability of the paving blocks to the sandbed only due to their dead weight.

These large areas of constant shear transfer to the sandbed (for the Concrete Interlocking Blocks) can be nicely seen in Fig. 11(f). Interestingly, between these areas and the load introduction zone where very high shear forces are introduced into the sandbed, an area with no force transmission becomes visible. A deeper look at the simulation results revealed that in these areas the paving blocks are lifted and, thus, are having no contact with the sandbed.

A far lesser impact of the type of paving block on the horizontal deformation was obtained for the stretcher bond laying pattern, as can be seen in Fig. 12. Clearly, this laying pattern allows for a natural distribution of the introduced load into the transverse direction for all types of paving blocks. This is illustrated by means of the nodal normal contact forces plotted in Fig. 13 for the Concrete Block superstructure.

Nevertheless, still a significant influence of the joint properties remains, leading to a 2.5 times higher deformation of the Concrete Block structure compared to the Double-T Block structure. Anyways, the appropriate choice of the size of the modelling region, to avoid a strong influence of the boundary conditions, can be seen well here. Only for the Double-T Block superstructure an even smaller maximum deformation would probably be obtained with a larger transverse modelling length.

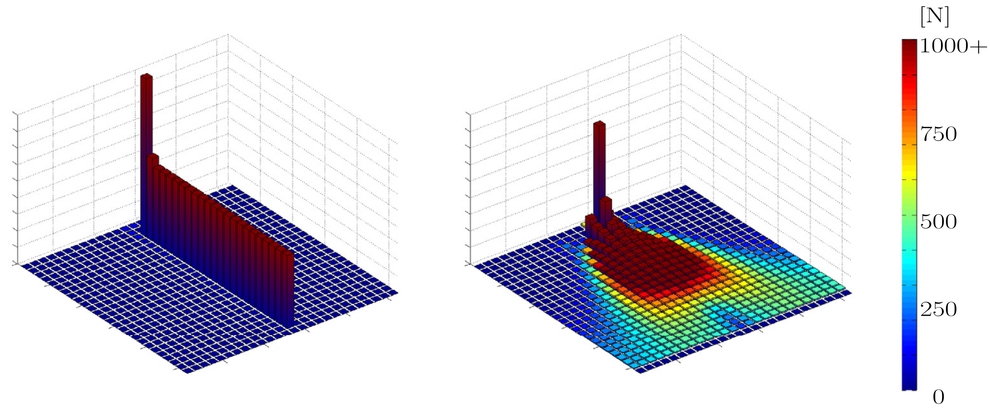

(a) Normal contact forces between Concrete Blocks

(b) Normal contact forces between Concrete Interlocking Blocks

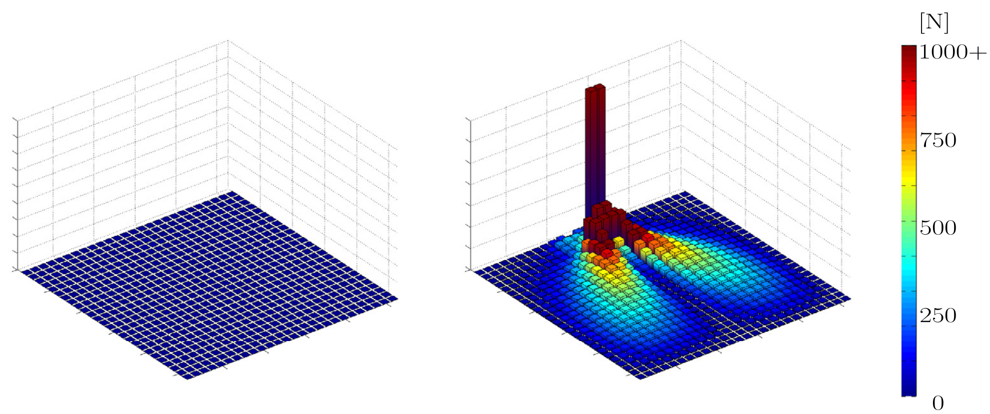

(c) Shear contact forces between Concrete Blocks

(d) Shear contact forces between Concrete Interlocking Blocks

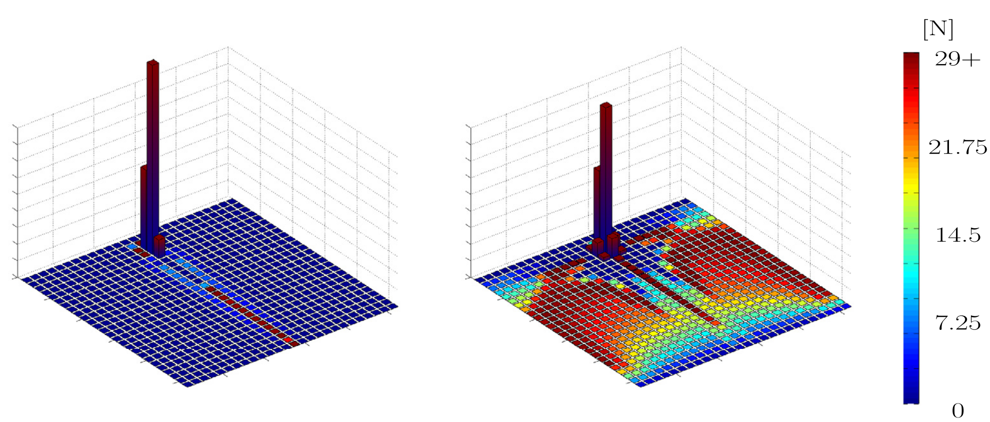

(e) Concrete Blocks: Shear contact forces in loading direction

(f) Concrete Interlocking Blocks: Shear contact forces in loading direction

Fig. 11. Visualisation of contact forces (in loading direction) between paving blocks, for the stacked bond laying pattern.

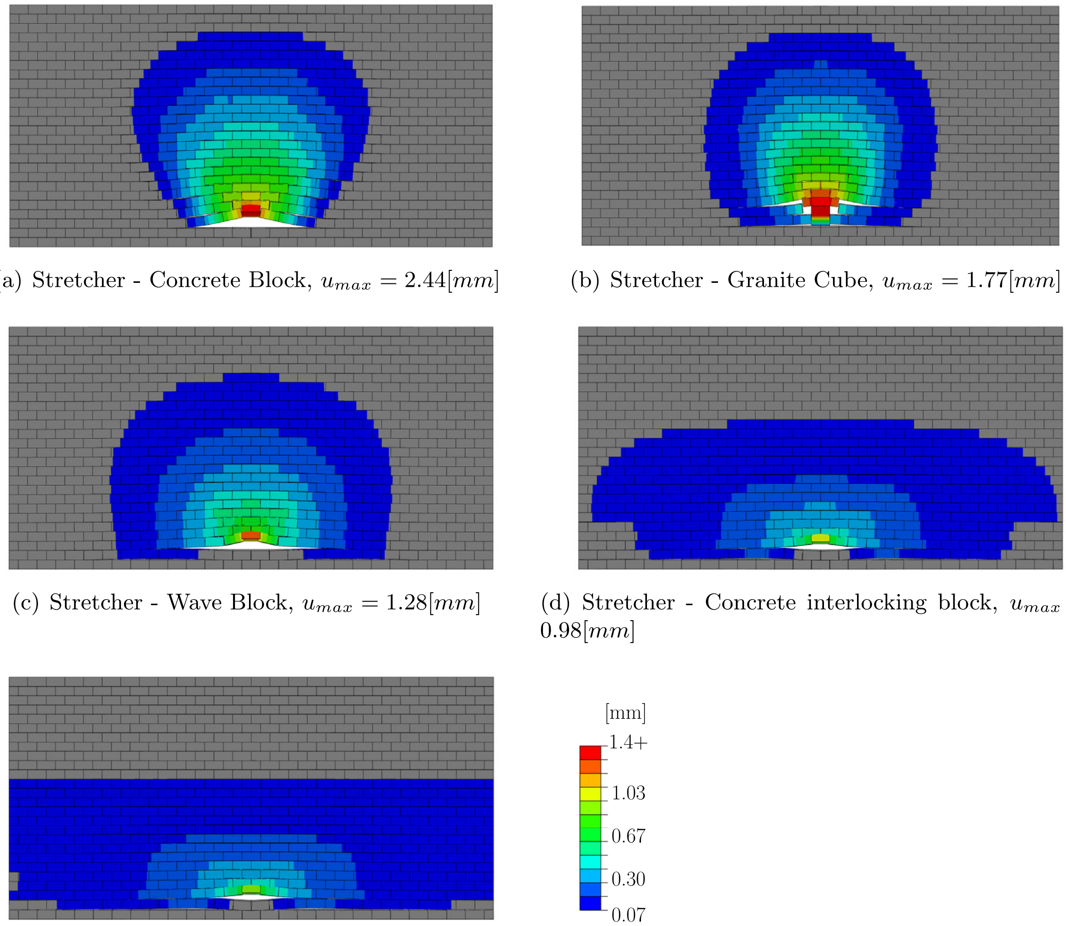

(a) Stretcher - Concrete Block, $u_{max} = 2.44[mm]$

(b) Stretcher - Granite Cube, $u_{max} = 1.77[mm]$

(c) Stretcher - Wave Block, $u_{max} = 1.28[mm]$

(d) Stretcher - Concrete interlocking block, $u_{max} = 0.98[mm]$

(e) Stretcher - Double-T Block, $u_{max} = 0.90[mm]$

Fig. 12. Horizontal deformation fields of the 5 investigated paving blocks arranged in a stretcher bond. A vertical and horizontal load of 57.5 kN each is introduced on one paving block. Scaling of deformations: 100.

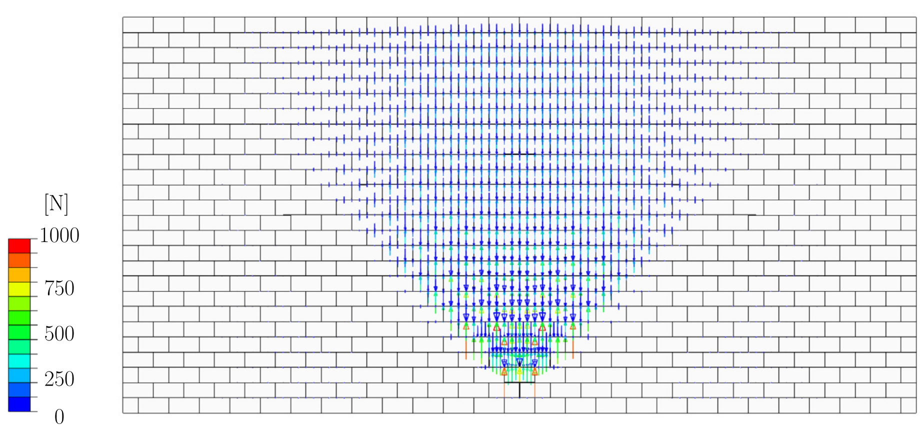

Fig. 13. Nodal normal contact forces in load direction for a stretcher bond with Concrete Blocks.

4.2. Performance of different laying patterns with the same paving blocks

In the following, horizontal deformation fields are shown for the 6 different laying patterns and for the Concrete Block as well as the Concrete Interlocking Block.

The results for the stacked bond, the stretcher bond, and the herringbone are illustrated in Fig. 14. Fig. 14(a) to (d) have already been shown before, but only in this comparison it becomes obvious that the stretcher bond represents the ideal laying pattern for conventional concrete paving blocks. The maximum horizontal deformation is only

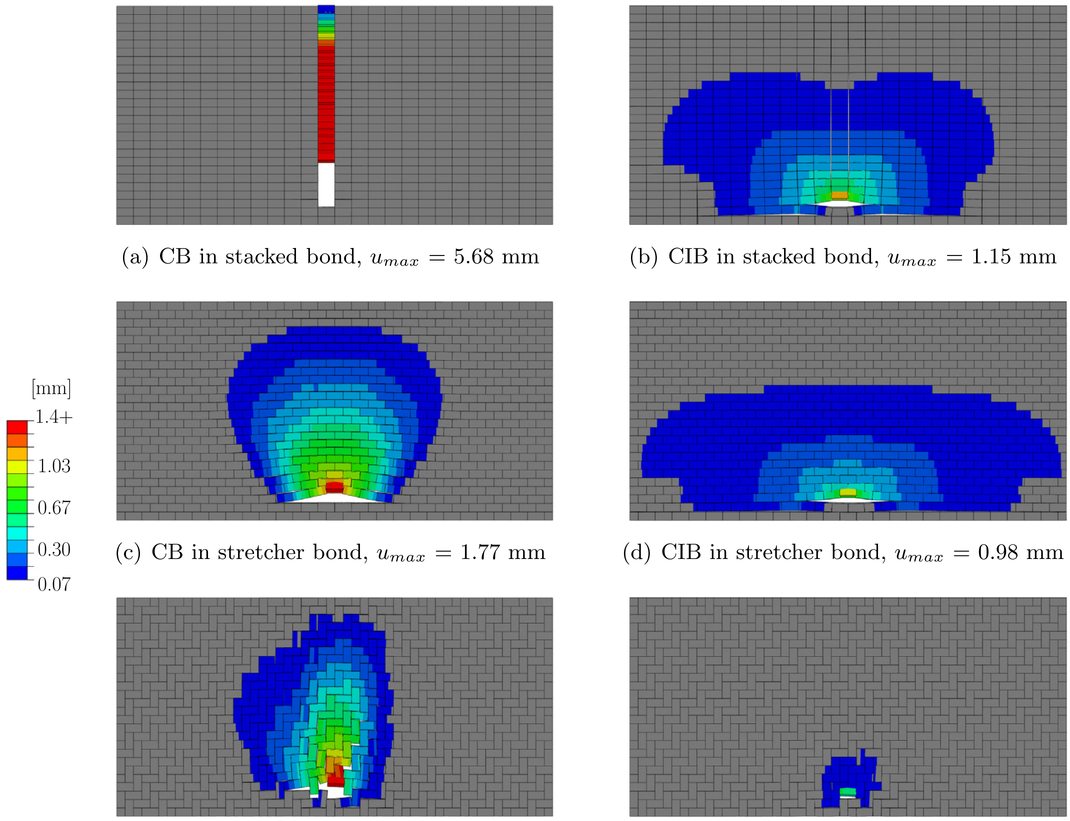

(a) CB in stacked bond, $u_{max} = 5.68$ mm
(b) CIB in stacked bond, $u_{max} = 1.15$ mm
(c) CB in stretcher bond, $u_{max} = 1.77$ mm
(d) CIB in stretcher bond, $u_{max} = 0.98$ mm
(e) CB in Herringbone, $u_{max} = 1.94$ mm
(f) CIB in Herringbone, $u_{max} = 0.64$ [mm]

Fig. 14. Horizontal deformation fields for three different laying patterns and two different paving blocks. A vertical and horizontal load of 57.5 kN each is introduced on one paving block. Scaling of deformations: 100.

slightly higher than that of the concrete block with interlocking effect in the stretcher bond, and it is smaller than the maximum deformation in all other laying patterns. Conversely, CIBs are ideally suited for a stacked bond, because their interlocking capabilities fully compensate the non-interlocking nature of this laying pattern.

It is also interesting to see that the performance of the Concrete Block is getting worse when laid in a herringbone laying pattern instead of a stretcher bond while the performance of the CIB is getting even better. This is because the interlocking capability of the herringbone can only be activated ideally if the vertical joints exhibit cohesive behaviour (as can be seen in Fig. 14(e) to (f)).

The deformation fields of the three remaining laying patterns, the 45° rotated ones, are shown in Fig. 15.

As can be seen, even for this complex arrangements of paving blocks the numerical simulation tool is able to deliver plausible shifting mechanisms. The mechanisms themselves are strongly characterized by the 45° orientation of the laying patterns. Looking at the conventional Concrete Block, only for the stacked bond a significant performance improvement can be identified compared to its not rotated counterpart, while for the other two laying patterns similar maximum deformations are obtained. For the stretcher bond an even worse performance can be observed, which is caused by a very concentrated, and thus bad, force distribution into the superstructure. This is illustrated in Fig. 16, showing the rather narrow bands of nodal normal contact forces in this laying pattern.

Considering the Concrete Interlocking Blocks, the performance is better for all three laying patterns. This has essentially two reasons: First, due to the 45° rotation more joints are heavily loaded by shear forces and, thus, the interlocking capability of the joints get highly activated and, secondly, also paving blocks behind the load introduction are getting involved in the load transfer mechanism.

4.3. Overview of simulation results

Fig. 17 finally shows the maximum horizontal deformation in loading direction u_{max} for all configurations of the 6 laying patterns with the 5 investigated paving blocks. In general it can be said that both the type of laying pattern and the type of paving block have a significant influence on the horizontal shifting resistance. However, disregarding the stacked bond, the paving block type seems to play a more important role and cannot be compensated by the type of laying pattern easily. On average paving blocks with joints providing a decent interlocking effect perform three times as good as paving blocks in the same laying pat-

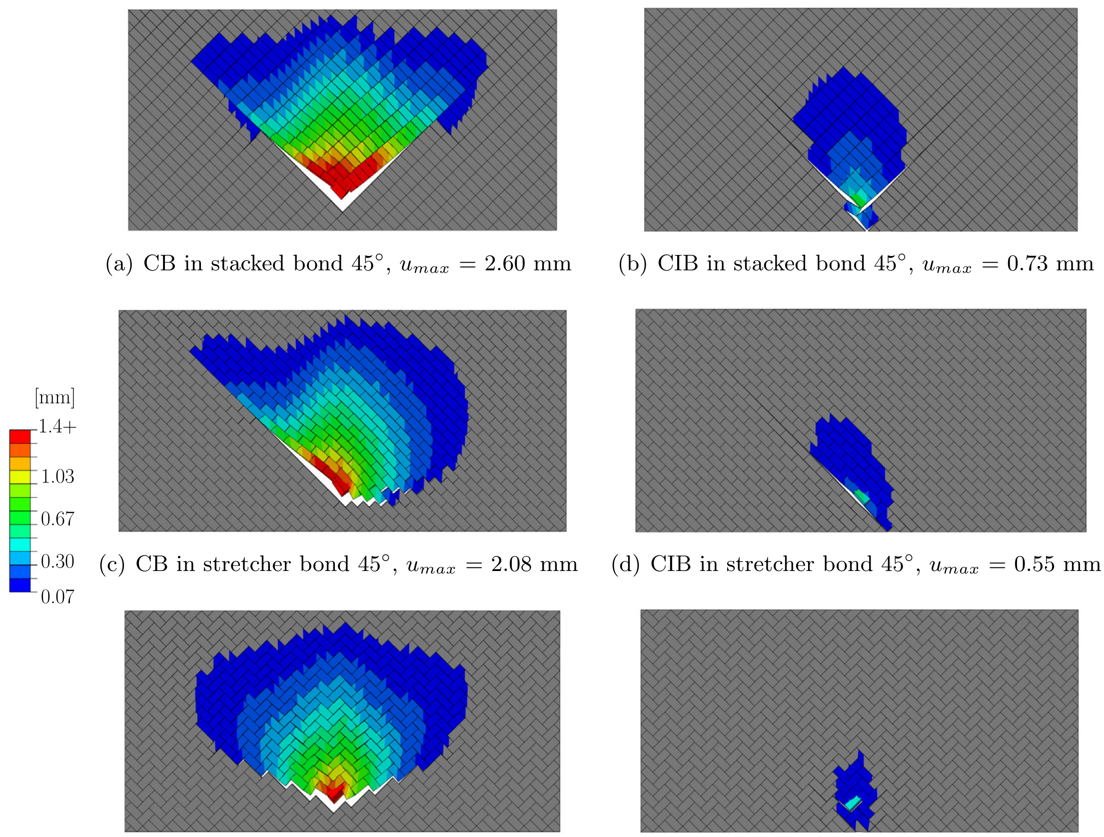

(a) CB in stacked bond 45°, $u_{max} = 2.60$ mm

(b) CIB in stacked bond 45°, $u_{max} = 0.73$ mm

(c) CB in stretcher bond 45°, $u_{max} = 2.08$ mm

(d) CIB in stretcher bond 45°, $u_{max} = 0.55$ mm

(e) CB in herringbone 45°, $u_{max} = 1.83$ [mm]

(f) CIB in herringbone 45°, $u_{max} = 0.47$ mm

Fig. 15. Horizontal deformation fields for three different laying patterns and two different paving blocks. A vertical and horizontal load of 57.5 kN each is introduced on one paving block. Scaling of deformations: 100.

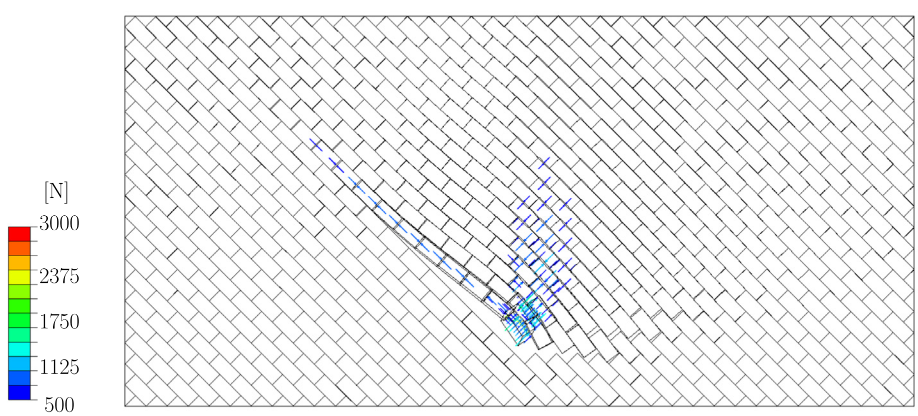

Fig. 16. Rather bad distribution of nodal normal contact forces in a stretcher bond 45° with Concrete Blocks, leading to high horizontal deformations.

tern without interlocking capabilities. This may lead to huge performance differences also in practical applications and shouldn't be ignored by design concepts and standards.

Of course, there are still a lot of other parameters influencing this horizontal deformation resistance, such as the paving block height, the joint filling (which can partly be described by the paving block height), the contact stiffness (which could be reduced in case of poorly compaction), and so on. The presented numerical simulation tool is capable of taking all this parameters into account. Two relationships are exemplarily given in Fig. 18, showing the significant influence of the paving block height as well as the normal contact stiffness in the vertical joints. A doubling of this stiffness can reduce the maximum horizontal deformation by almost half.

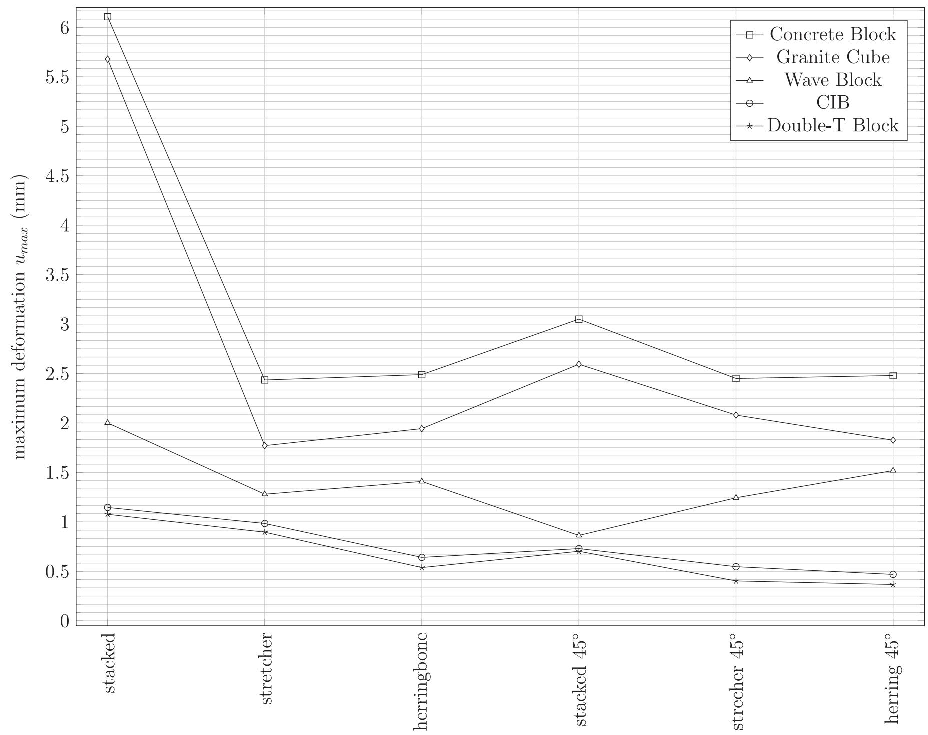

Fig. 17. Maximum horizontal deformation in loading direction u_{max} for the investigated 6 different laying patterns and 5 different paving blocks.

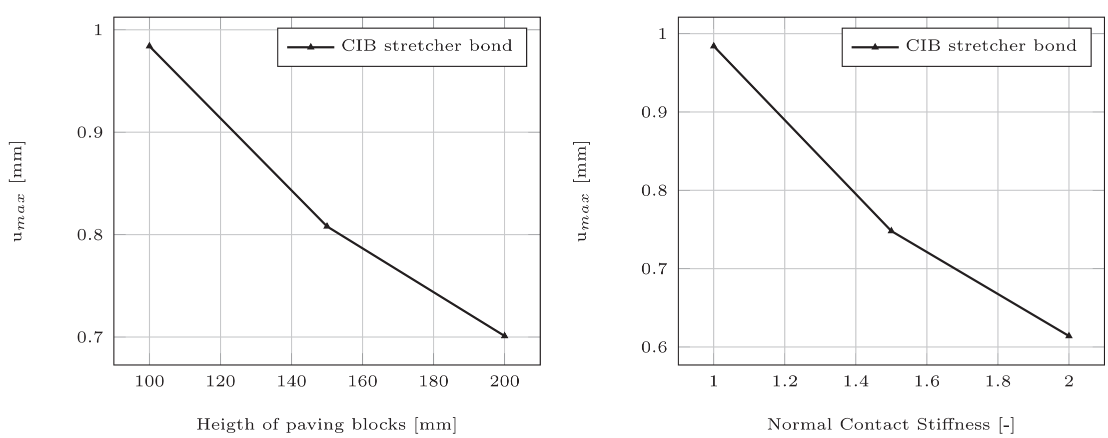

Fig. 18. Influence of the paving block height and contact stiffness in normal direction on the maximum horizontal deformation.

5. Conclusions

In this paper, a numerical simulation tool has been proposed allowing for a realistic reproduction of resistance mechanisms of paving block superstructures under horizontal loading. To accomplish that, numerical models with more than 2000 non-linear interactions, with their behaviour defined through a user subroutine written in Fortran, had to be run. The required strength properties to define the non-linear joint behaviour of all five investigated paving block types were obtained by special tangential shear experiments. Based on these investigations, answers to the three questions raised in the introduction can now be formulated:

- The fully automation of the model creation, enabled by a complex Python script, allowed us to run a huge amount of simulations to finally identify an appropriate model size for which the influence of boundary conditions is not significant for the majority of the investigated configurations. Furthermore, much attention was paid to any kind of numerical regularisation mechanism, like artificial stiffness and viscous damping. Many parameters studies were conducted to ensure that such influences are negligible.
- The non-linear behaviour of the vertical joints, in normal as well as tangential direction, could be reproduced quite accurately. Therefore, information from two kind

of joint experiments were used and implemented into the numerical simulation tool.
- Mainly for this reason, very plausible 3D deformation mechanisms could be obtained for several laying patterns with different types of paving blocks. Interesting insights into load transfer mechanisms could be gained, showing a huge variety depending on the combination of laying pattern, type of paving block and the related joint behaviour. Finally, this allowed for a comprehensive performance evaluation of several paving block pavements with respect to their horizontal deformation resistance.

In short, the simulation results have confirmed the high performance expectations of paving blocks with interlocking effects. On average these paving blocks perform three times as good as blocks without interlocking capabilities, considering the same laying pattern. Even for the stacked bond laying pattern, where no structural load distribution occurs, paving blocks with interlocking effect can lead to reasonable horizontal deformation resistances. Furthermore, as the horizontal deformation in those superstructures is highly affected by the stiffness of their sand-filled joints, it should be ensured that these joints are completely filled, well compacted, and their width and quantity minimized.

In summary, this work has the intention to demonstrate the very different horizontal resistance of paving block pavements, to propose a method to identify this resistance, and to possibly contribute to future design concepts which will hopefully cover this type of damage scenario. To increase the computational efficiency of such kind of calculations, the application of finite-element-based limit analysis formulations, as presented in Li et al. [18] for orthotropic strength behaviour and in Li et al. [19] including discontinuities, could be a possible future step.

References

[1] T. Nishizawa, S. Matsuno, M. Komura, Analysis of Interlocking Block Pavements by Finite Element Method, International Conference on Concrete Block Paving, 1984.

[2] M. Jacobs, L. Houben, Wheel Testing and Finite Element Analysis of Concrete Block Pavement, Delft University of Technology, The Netherlands, 1988.

[3] M. Huurman, L.J.M. Houben, A.W.M. Kok, Development of a three-dimensional finite element model for concrete block pavements, in: Proceedings Fourth International Conference on Concrete Block Paving, 1992.

[4] A. Hassani, Modelling and Structural Design of a Concrete Block Pavement System, International Conference on Concrete Block Paving, 2006.

[5] T. Lerch, Investigation of the Deformation Behaviour of Concrete Block Pavements under Simulated Traffic Loading (Ph.D. thesis), TU Dresden, 2005.

[6] D. Ascher, T. Lerch, M. Oeser, F. Wellner, 3d-fem Simulation of Concrete Block Pavement, Int. Conference on Concrete Block Paving, 2006.

[7] F.M. Nejad, M.R. Shadravan, A Study on Behavior of Block Pavement using 3d Finite Element Method, International Conference on Concrete Block Paving, 2006.

[8] W.K. Mampearachchi, W.P.H. Gunarathna, Finite-element model approach to determine support conditions and effective layout for concrete block paving, J. Mater. Civ. Eng. (2010)

[9] M. Oeser, H. Chandra, Segmented concrete block pavements: analysis with optimized numerical tool, 2010.

[10] J. Füssl, W. Kluger-Eigl, R. Blab, Mechanical performance of pavement structures with paving slabs–Part I: full-scale accelerated tests as validation for a numerical simulation tool, Eng. Struct. 98 (2015) 212–220, https://doi.org/10.1016/j.engstruct.2014.10.054.

[11] J. Füssl, W. Kluger-Eigl, L. Eberhardsteiner, R. Blab, Mechanical performance of pavement structures with paving slabs–Part II: numerical simulation tool validated by means of full-scale accelerated tests, Eng. Struct. 98 (2015) 221–229, https://doi.org/10.1016/j.engstruct.2014.10.055.

[12] J. Füssl, H. Hengl, L. Eberhardsteiner, W. Kluger-Eigl, R. Blab, Numerical simulation tool for paving block structures assessed by means of full-scale accelerated pavement tests, Int. J. Pavement Eng. (2016) 1–13, https://doiorg/10.1080/10298436.2016.1224410.

[13] H. Hengl, J. Füssl, The influence of superelevated profiles of paving block structures on their load-bearing behavior, Eng. Struct. 117 (2016) 195–203, https://doi.org/10.1016/j.engstruct.2016.03.003.

[14] H. Hengl, W. Kluger-Eigl, R. Blab, J. Füssl, The performance of paving block structures with mortar filled joints under temperature loading, accessed by means of numerical simulations, Road Mater. Pavement Des. (2017) 1–20, https://doiorg/10.1080/14680629.2017.1330221.

[15] M. Rachmat, M.N. Hasanan, R.H. Mohd, L. Tung-Chai, Performance of concrete block pavement on sloped road section, Int. J. Pavement 6 (1) (2007) 136–145.

[16] J. Füssl, W. Kluger-Eigl, R. Blab, Experimental identification and mechanical interpretation of the interaction behaviour between concrete paving blocks, Int. J. Pavement Eng. 17 (2016) 478–488, https://doi.org/10.1080/10298436.2014.993205.

[17] D.S.S. Corp., Abaqus Analysis User's Manual, Providence, 2016.

[18] M. Li, J. Füssl, M. Lukacevic, J. Eberhardsteiner, C. Martin, Strength predictions of clear wood at multiple scales using numerical limit analysis approaches, Comput. Struct. 196 (2018) 200–216, https://doi.org/10.1016/j.compstruc.2017.11.005.

[19] M. Li, J. Füssl, M. Lukacevic, J. Eberhardsteiner, C. Martin, A numerical upper bound formulation with sensibly-arranged velocity discontinuities and orthotropic material strength behaviour, J. Theoret. Appl. Mech. 56 (2018) 417–433, https://doi.org/10.15632/jtam-pl.56.2.417.